HHS Public Access

Author manuscript

J Phys Chem Lett. Author manuscript; available in PMC 2017 August 04.

Published in final edited form as:

J Phys Chem Lett. 2016 August 4; 7(15): 3046–3051. doi:10.1021/acs.jpclett.6b01172.

Fluorescence from Multiple Chromophore Hydrogen-Bonding States in the Far-Red Protein TagRFP675

Patrick E. Konold[1,2], **Eunjin Yoon**[3], **Junghwa Lee**[3], **Samantha Allen**[1,2], **Prem P. Chapagain**[4], **Bernard S. Gerstman**[4], **Chola K. Regmi**[4,5], **Kiryl D. Piatketvich**[6], **Vladislav V. Verkhusha**[7], **Taiha Joo**[3], and **Ralph Jimenez**[1,2,*]

[1]JILA, University of Colorado and NIST, Boulder, CO 80309

[2]Department of Chemistry & Biochemistry, University of Colorado, Boulder, CO 80309

[3]Department of Chemistry, Pohang University of Science and Technology (POSTECH), Pohang, South Korea 790-784

[4]Department of Physics, Florida International University, Miami, FL 33199

[5]Department of Physics, Virginia Tech, Blacksburg, VA 24061

[6]Massachusetts Institute of Technology Media Lab, Massachusetts Institute of Technology, Cambridge, MA 02139

[7]Department of Anatomy & Structural Biology, Albert Einstein College of Medicine, Bronx, NY 10461

Abstract

Far-red fluorescent proteins are critical for *in vivo* imaging applications, but the relative importance of structure versus dynamics in generating large Stokes-shifted emission is unclear. The unusually red-shifted emission of TagRFP675, a derivative of mKate, has been attributed to the multiple hydrogen bonds with the chromophore N-acylimine carbonyl. We characterized TagRFP675 and point mutants designed to perturb these hydrogen bonds with spectrally-resolved transient grating and time-resolved fluorescence (TRF) spectroscopies supported by molecular dynamics simulations. TRF results for TagRFP675 and the mKate/M41Q variant show ps timescale red-shifts followed by ns time blue-shifts. Global analysis of the TRF spectra reveals spectrally-distinct emitting states that do not interconvert during the S_1 lifetime. These dynamics originate from photoexcitation of a mixed ground state population of acylimine hydrogen bond conformers. Strategically tuning the chromophore environment in TagRFP675 might stabilize the most red-shifted conformation and result in a variant with a larger Stokes shift.

Keywords

Red fluorescent protein; Protein dynamics; Femtosecond spectroscopy

*Correspondence should be addressed to R.J. (rjimenez@jila.colorado.edu) or T.J. (thjoo@postech.ac.kr) .

Supporting Information

Experimental and computational methods, additional data and analysis results for SRTG and TRF are provided in Supporting Information. This information is available free of charge on the Internet at www.pubs.acs.org.

Red FPs (RFPs) with excitation and emission wavelengths beyond 650 nm (15380 cm^{-1}) are eagerly sought for *in vivo* imaging because they offer the prospect of lower autofluorescence background, lower light scattering, and higher tissue transmission relative to shorter-wavelength fluorophores.[1-4] Accordingly, molecular engineering of new RFPs with large Stokes-shifted emission is an important topic. Hydrogen-bonding to the *N*-acylimine carbonyl of the chromophore has been observed in the most red-emitting RFPs, including mNeptune, mCardinal, eqFP650, eqFP670, mRojoA, mRouge, and mPlum.[5-11] The reddest-emitting GFP-like protein with a reported crystal structure, TagRFP675,[9], [12-13] contains an N-acylimine carbonyl with two hydrogen bonds, neither of which is present in its predecessor mKate (Figure 1). One arises from a direct interaction with the Q41 sidechain, while the other involves a water molecule supported by tertiary interactions with the amide group of Q106.

Although hydrogen bonding to the N-acylimine carbonyl is strongly correlated with a large Stokes shift, the mechanism is still in question. We previously investigated mPlum, which has only a single hydrogen bond at this position. [14,15-16] Utilizing Spectrally-Resolved Transient Grating (SRTG) spectroscopy and Molecular Dynamics (MD) simulations on a series of point mutants, we found that its red-shifted emission correlates with ps-timescale switching between direct and water-mediated E16-I65 hydrogen-bonding interactions.[14] Faraji and Krylov explained this effect with QM/MM calculations revealing the electron density increase at the carbonyl oxygen in S_1, and the relatively better electron accepting ability of a water-mediated hydrogen bond relative to a direct interaction with E16.[17] More recent femtosecond time-resolved fluorescence spectra (TRFS) revealed a 37 ps timescale for excited-state interconversion between the direct and water-mediated hydrogen-bonding structures.[18] We now report the excited-state dynamics of TagRFP675 investigated with SRTG and TRFS measurements and MD simulations. The fluorescence dynamics are explained in terms of heterogeneous emission resulting from distinct acylimine hydrogen-bonding structures.

One set of TagRFP675 mutants was designed to perturb the water-mediated hydrogen bond between Q106 and F62. The Q106M mutation disrupts the interaction by replacing one of the participating sidechains with a group of similar size without a hydrogen-bond donor, whereas the F62A mutation alters the sterics, as was previously demonstrated for mPlum.[14] To probe the Q41 interaction, we added this hydrogen-bonding group to the parent mKate (*i.e.* mKate/M41Q), and removed it from TagRFP675 (*i.e.* TagRFP675/Q41M). Absorption peaks of these variants (Table 1) fall between 16670-17090 cm^{-1} (585-600 nm). As expected, disruption of the water-mediated hydrogen bond network by single or double point mutations leads to blue-shifted emission in the TagFP675/F62A, Q106M, and F62A/Q106M variants. Addition of a hydrogen bond at the N-acylimine carbonyl in mKate/M41Q leads to a 700 cm^{-1} increase in Stokes shift, while its removal in TagRFP675/Q41M yields a 460 cm^{-1} decrease.

SRTG measurements were employed to characterize ground and excited state dynamics of the RFPs. The transient spectral features shown in the contour plots of Figure 2a and 2b for TagRFP675 and mKate/M41Q correspond to the Ground State Bleach (GSB) and Stimulated

Emission (SE) responses. SRTG spectra of the other RFPs (Figure S2) show a similar bimodal shape, except for TagRFP675/Q41M and mKate, where the SE contribution is only present as a shoulder on the GSB peak. The SE contribution was fitted to a Gaussian function, and the peak frequency versus time shows a red-shift with biexponential kinetics with, for example 17 ps and 397 ps components for TagRFP675, and a total spectral shift of 77 cm^{-1}. Parameters for the other RFPs are given in Table S1. Notethat SRTG differs from transient absorption in that the third-order optical response is detected in quadrature and as a consequence SRTG signals are positive and time evolution of the intensity is twice as fast.[19] Time constants reported in Figure 2 and Tables S1 and S2 are corrected accordingly. This transient red-shift is consistent with excited-state solvation dynamics, although the magnitude of the observed shift is much smaller than the total Stokes shift due to the limited excitation bandwidth and the presence of an overlapping ESA band as discussed previously for mPlum.[14] Global analysis revealed the SRTG are well fit by three components with timescales ranging from a few ps to almost 2 ns (Figures 2 and S3 and Table S2). The amplitudes of all Decay Associated Spectra (DAS) components extend over both the GSB and SE bands, indicating that the transitions are largely overlapped. In all cases, amplitudes of the DAS are positive at all wavelengths, indicating that only decay components and no risetimes are observed. The SE peak shifts are therefore not due to a spectral red-shift as expected from conventional solvation dynamics, but instead are caused by the lifetime decays of multiple spectral forms.

To further evaluate the dynamics of TagRFP675 and mKate/M41Q we employed TRFS. Time-Resolved Area-Normalized Spectra (TRANES) of these RFPs are shown in Figure 3. These data sets are comprised of spectra from fluorescence upconversion for time delays < 1 ns stitched together with spectra from time-correlated single photon counting for longer times (methods described in Supporting Information). Although TRFS often reveal transient red-shifts associated with solvation dynamics, these RFPs show atypical behavior. The total spectral shifts are only a small proportion of their total Stokes shifts, and, most unusually, the time-evolution of the first moments show initial red-shifts followed by ns timescale blue-shifts (Figure S5 and fit parameters collected in Table S3). Although neither RFP shows an isoemissive point at all times, both show an isoemissive point for part of the experimental time window. This spectral behavior is a hallmark of a system with a small number of discrete emitting states.[20] For TagRFP675, TRANES show an isoemissive point near 15000 cm^{-1} at times less than ~100 ps (Figure 3a), whereas mKate/M41Q (Figure 3c) shows isoemissive behavior at very short times, < 1 ps.

The DAS of TagRFP675 from global analysis fitting of the TRFS (Figure 4a) consists of four components, whereas mKate/M41Q (Figure 4b) shows three components. For both RFPs, the components are decays at all wavelengths, which means that no population redistribution occurs, and the mixture of spectral forms in S_1 therefore results from the excitation of a mixed S_0 population. In both cases, there is a segregation of timescales between the fastest dynamics and the two longest components, which are of the largest amplitudes. Also, in both FPs, the longest lifetime is not associated with the most red-shifted state, which explains the origin of the ns-timescale blue shifts. The presence of the isoemissive points in both FPs is a result of a segregation in timescales. For mKate/M41Q, the 24 ps component is much faster than the 560 ps and 3.2 ns components which constitute

the majority of the emission decay. At early times, this system appears to be nearly two-state, and therefore shows an isoemissive point. Similar behavior is observedin TagRFP675.

Since the DAS of TagRFP675 and mKate/M41Q imply that multiple spectral forms originate in the ground state, we performed 50 ns classical MD simulations (described in Supporting Information) to determine if they show a small number of acylimine hydrogen-bond structures that could explain these spectral states. Figure 5a,b display the time trajectories of the distance (Δr), between the nitrogen atom in the Q41 sidechain and the N-acylimine carbonyl oxygen of F62 for both RFPs. Both variants largely maintain a conformation with a direct hydrogen bond (~3.5 Å), with rare excursions into a water-mediated structure (~4.5 Å) or non-hydrogen-bonded state ($\gtrsim$5 Å). The interaction between F62 and Q106, which is the other immediate interaction, showed contrasting behavior for the two FPs. In TagRFP675, the water molecule is mobile and moves into a water-mediated hydrogen bond with Q41. However, in mKate/M41Q, the Q106-F62 hydrogen bond is more stable, and this water molecule never leaves. Neither RFP shows a direct F62-Q106 hydrogen bond during the 50 ns trajectories.

The S28-Q41 hydrogen bond plays an important role in orienting the Q41 sidechain for its interaction with F62. In TagRFP675 (Figure 5d,f), this interaction converts between three states, whereas mKate/M41Q converts between two states (Figure 5e,f). For the dominant configuration in TagRFP675 (Figure 6a), S28 hydrogen bonds with Q41. In another orientation, it hydrogen bonds to R42, resulting in two structures. In one, the Q41 amino group interacts with S28 via a water-mediated hydrogen bond (Figure 6b) while the other is a water-mediated hydrogen bond with the carbonyl (Figure 6c). Both structures result in an extended network: F62-Q41-water-S28-R42 involving a water molecule that more frequently hydrogen-bonds between F62 and Q106. The S28 and Q41 sidechain dynamics, along with this mobile water molecule, lead to a highly dynamic network in TagRFP675. Only two structures are observed for mKate/M41Q. In both, a water molecule is found between F62 and Q106. The dominant structure contains a direct S28-Q41 carbonyl interaction (Figure 6d), whereas another contains S28 interacting directly with both Q41 and R42 (Figure 6e). Figure 6 shows the percentage of time spent in each of these conformations during the 50 ns trajectory.

The SRTG and TRF results on TagRFP675 and mKate/M41Q both reveal multiple ps/ns components, and more significantly, neither measurement reveals rise-times. The excitation and detection conditions of the two experiments differ, and consequently prepare and probe different mixtures of spectral forms. SRTG was performed with large bandwidth pulse spectra in which excitation and detection spans the red-edge of the absorption and part of the emission spectra (Figure S1). The excitation spectrum therefore creates a hole in the absorption spectrum. Because the system is inhomogeneously broadened due to the multiple ground-state spectral components, the SE band does not significantly red shift, and the GSB component does not significantly blue-shift. In contrast, TRF was performed with narrow-band excitation spectra near the peak absorption wavelength and wide-band, spectrally-resolved detection. Nevertheless, results from both measurements consistently point to the parallel decay of an optically excited set of states. Additional support for the presence of multiple ground states is provided by steady-state fluorescence measurements on both FPs

(Supporting Information Figure S6) showing that the emission peak wavelength varies as excitation wavelength is tuned across the absorption band.[9]

Our model of the fluorescence dynamics is based on the TRFS global analysis results, which permits a complete view of the emitting states. For a mixture of non-interconverting emitting states with distinct lifetimes, the spectrum of each component can be obtained from the DAS. Since the analysis reveals well-separated decay time constants, we expect that the DAS components correspond to distinct spectral states. The peak energy and relative weight of each component is taken from the DAS, assuming equal excitation probabilities. The resulting diagrams (Figure 7a,b) depict the photoexcitation of a mixture of ground states, creating a set of four emitting states in the case of TagRFP675 and three states for mKate/M41Q. The >500 ps components represent the predominant emitting states of each FP, and are consistent with the measured fluorescence lifetimes.[9, 12-13]

Next, we consider possible structural origins of these spectral forms. The SRTG and steady-state spectra show that perturbation of the water-mediated hydrogen bond between Q106 and the acylimine in the TagRFP675/F62A, Q106M, and F62A/Q106M mutants leads to a moderate decrease (~300 cm^{-1}) in Stokes shift and a minor effect on the excited-state timescales. These differences may be attributed to a change in flexibility of the acylimine carbonyl given a reduction in steric hindrance of the sidechain in the F62A mutation and loss of the water-mediated hydrogen bond in the Q106M mutation. The SRTG data also reveal that variants lacking a direct hydrogen bond to the Q41 sidechain (mKate, TagRFP675/Q41M) do not show ps/ns dynamics. In contrast, the presence of a hydrogen-bond donor to the acylimine in mKate/M41Q leads to a dramatically larger Stokes shift on par with TagRFP675 and similar excited-state timescales. It seems likely that the Q41-S28 interaction both indirectly modulates the hydrogen bond strength of Q41-F62 and modulates the flexibility of an extended network that interconverts between states. These results indicate that the direct hydrogen bond with the Q41 sidechain along with an extended hydrogen bond network has the largest impact on the Stokes shift of TagRFP675. We therefore suggest that the spectral forms identified in the DAS originate from distinct structures of the F62-Q41-S28 hydrogen-bonding network such as those illustrated in Figure 6. It is tempting to make specific assignments of these spectral forms to structures by relying on the amplitudes of the DAS spectra from TRF and the populations from the ground-state MD simulation. However, these assignments are likely to be inaccurate because at least the photoexcitation probability for each spectral form under the excitation wavelength and bandwidth needs to be taken into account. To produce reliable assignments, temperature and excitation wavelength-dependent TRF measurements are necessary and will be the subject of future research.

It is remarkable that small changes in hydrogen-bonding result in a 100-fold variation in excited-state lifetime. Understanding this effect will be critical for designing RFPs with high fluorescence yields, especially in light of the low brightness of most RFPs with large Stokes shifts.[21] Although our results emphasize the importance of the acylimine region for the Stokes shift, hydrogen-bonding to the chromophore p-hydroxyphenyl group also impacts the fluorescence properties. We also examined these interactions in our MD simulations of TagRFP675, mKate/M41Q, and mKate and find they are very similar. In all three FPs, the phenolate interacts predominantly with E141 via two water-mediated hydrogen bonds,

though interaction with N143 to a minor extent is also observed. Three movies showing hydrogen bonds in the phenolate and acylimine regions are provided in the Supporting Information. Since the dynamics are very similar for three RFPs with widely varying Stokes shift, it appears that interactions of the phenolate do not play a major role in the Stokes shift, but instead their role is to stabilize the fluorescent cis-conformation of the chromophore. A previous study of TagRFP675 reveal pH-dependent changes involving protonation of the p-hydroxyphenyl group and rearrangements of the N143, N158, and R197 sidechains. Furthermore, the fluorescence blue-shifts and the intensity decreases several-fold when the pH is decreased, with a midpoint near pH 5.5.[9] For the pH 8.0 buffer employed in the current study (which differs from that used in ref. 9), the TagRFP675 sample will contain a small percentage of the non-fluorescent structure. We propose that this alternate hydroxyphenyl structure corresponds to the 3.7 ps, blue-shifted state in Fig 7.

The dynamics of TagRFP675 are strikingly different from those of mPlum, which shows simple two-state emission behavior.[18] QM/MM calculations on mPlum show that the partial charge of the acylimine oxygen increases upon electronic excitation, and that the S_1 energy of the water-mediated hydrogen bonded state is below that of the direct hydrogen-bonded state.[17] When the mixed population of direct and water-mediated conformers in S_0 is photoexcited, the direct sub-population relaxes (on a 37 ps timescale) to a water-mediated state with lower energy, whereas the water-mediated population only slightlyre organizes. In contrast, the presence of two acylimine-sidechain interactions in TagRFP675 leads to several different hydrogen bond conformations in S_0, which unlike in mPlum, do not convert to a dominant configuration in S_1. Another point of contrast is that the most frequent reconfiguration of the hydrogen bond network observed in MD does not involve immediate hydrogen bonding to the acylimine, but rather the secondary set of interactions with the Q41 sidechain. These hydrogen bond rearrangements could impact the electronic energies by influencing the orientation of the Q41 hydrogen-bond donating groups to the acylimine carbonyl, in turn modulating the electron-accepting capability of the donor groups.

In conclusion, our central finding is that the presence of two acylimine hydrogen-bonding interactions in TagRFP675 and mKate/M41Q leads to a heterogeneous system with multiple emitting forms that do not interconvert on the timescale of the S_1 lifetime. The absence of a continuous solvation process with amplitude of red-shift comparable to the total Stokes shift of TagRFP675 implies that the environment is fairly rigid, and only permits energetically significant relaxation along degrees of freedom involving the hydrogen bonds near the acylimine. We suggest that the majority of the Stokes shift in TagRFP675 and mKate/M41Q occurs *via* sub-ps chromophore relaxation which is not observed in the current measurements due to insufficient time resolution, though such dynamics were proposed to be the origin of a 160 fs timescale observed in mPlum.[18] Another important finding is that the most red-shifted component (530 ps lifetime) in the DAS of TagRFP675 peaks at 680 nm. Strategically tuning the chromophore environment to stabilize the conformation corresponding to this spectral form would yield an improved longer wavelength emitting RFP for *in vivo* imaging.

Supplementary Material

Refer to Web version on PubMed Central for supplementary material.

Acknowledgements

This work was supported by the NSF Physics Frontier Center at JILA and the National Institutes of Health (GM105997 and GM108579 to V.V.V and SC3GM096903 to PC). S.A. was supported by the University of Colorado Molecular Biophysics Training Grant (T32 GM065103). TJ acknowledges the financial support by the Global Research Laboratory Program (2009-00439) through the National Research Foundation of Korea. R.J. is a staff member in the Quantum Physics Division of the National Institute of Standards and Technology (NIST). Certain commercial equipment, instruments, or materials are identified in this paper in order to specify the experimental procedure adequately. Such identification is not intended to imply recommendation or endorsement by the NIST, nor is it intended to imply that the materials or equipment identified are necessarily the best available for the purpose.

References

1. Wu B, Piatkevich KD, Lionnet T, Singer RH, Verkhusha VV. Modern Fluorescent Proteins and Imaging Technologies to Study Gene Expression, Nuclear Localization, and Dynamics. Current Opinion in Cell Biology. 2011; 23:310–317. [PubMed: 21242078]
2. Shcherbakova DM, Subach OM, Verkhusha VV. Red Fluorescent Proteins: Advanced Imaging Applications and Future Design. Angewandte Chemie-International Edition. 2012; 51:10724–10738.
3. Chudakov DM, Matz MV, Lukyanov S, Lukyanov KA. Fluorescent Proteins and Their Applications in Imaging Living Cells and Tissues. Physiological Reviews. 2010; 90:1103–1163. [PubMed: 20664080]
4. Subach FV, Piatkevich KD, Verkhusha VV. Directed Molecular Evolution to Design Advanced Red Fluorescent Proteins. Nature Methods. 2011; 8:1019–1026. [PubMed: 22127219]
5. Lin MZ, McKeown MR, Ng H-L, Aguilera TA, Shaner NC, Campbell RE, Adams SR, Gross LA, Ma W, Alber T, Tsien RY. Autofluorescent Proteins with Excitation in the Optical Window for Intravital Imaging in Mammals. Chemistry & Biology. 2009; 16:1169–1179. [PubMed: 19942140]
6. Chu J, Haynes RD, Corbel SY, Li P, Gonzalez-Gonzalez E, Burg JS, Ataie NJ, Lam AJ, Cranfill PJ, Baird MA, Davidson MW, Ng H-L, Garcia KC, Contag CH, Shen K, Blau HM, Lin MZ. Non-Invasive Intravital Imaging of Cellular Differentiation with a Bright Red-Excitable Fluorescent Protein. Nature Methods. 2014; 11:572–578. [PubMed: 24633408]
7. Pletnev S, Pletneva NV, Souslova EA, Chudakov DM, Lukyanov S, Wlodawer A, Dauter Z, Pletnev V. Structural Basis for Bathochromic Shift of Fluorescence in Far-Red Fluorescent Proteins eqFP650 and eqFP670. Acta Crystallographica Section D-Biological Crystallography. 2012; 68:1088–1097.
8. Chica RA, Moore MM, Allen BD, Mayo SL. Generation of Longer Emission Wavelength Red Fluorescent Proteins Using Computationally Designed Libraries. Proceedings of the National Academy of Sciences of the United States of America. 2010; 107:20257–20262. [PubMed: 21059931]
9. Piatkevich KD, Malashkevich VN, Morozova KS, Nemkovich NA, Almo SC, Verkhusha VV. Extended Stokes Shift in Fluorescent Proteins: Chromophore-Protein Interactions in a near-Infrared TagRFP675 Variant. Scientific Reports. 2013; 3
10. Wang L, Jackson WC, Steinbach PA, Tsien RY. Evolution of New Nonantibody Proteins Via Iterative Somatic Hypermutation. Proceedings of the National Academy of Sciences of the United States of America. 2004; 101:16745–16749. [PubMed: 15556995]
11. Li Z, Zhang Z, Bi L, Cui Z, Deng J, Wang D, Zhang X-E. Mutagenesis of mNeptune Red-Shifts Emission Spectrum to 681-685 Nm. Plos One. 2016; 11
12. Shcherbo D, Merzlyak EM, Chepurnykh TV, Fradkov AF, Ermakova GV, Solovieva EA, Lukyanov KA, Bogdanova EA, Zaraisky AG, Lukyanov S, Chudakov DM. Bright Far-Red Fluorescent Protein for Whole-Body Imaging. Nature Methods. 2007; 4:741–746. [PubMed: 17721542]

13. Morozova KS, Piatkevich KD, Gould TJ, Zhang J, Bewersdorf J, Verkhusha VV. Far-Red Fluorescent Protein Excitable with Red Lasers for Flow Cytometry and Superresolution Sted Nanoscopy. Biophysical Journal. 2010; 99:L13–L15. [PubMed: 20643047]
14. Konold P, Regmi CK, Chapagain PP, Gerstman BS, Jimenez R. Hydrogen Bond Flexibility Correlates with Stokes Shift in mPlum Variants. The Journal of Physical Chemistry B. 2014; 118:2940–8. [PubMed: 24611679]
15. Abbyad P, Childs W, Shi X, Boxer SG. Dynamic Stokes Shift in Green Fluorescent Protein Variants. Proceedings of the National Academy of Sciences of the United States of America. 2007; 104:20189–20194. [PubMed: 18077381]
16. Shu X, Wang L, Colip L, Kallio K, Remington SJ. Unique Interactions between the Chromophore and Glutamate 16 Lead to Far-Red Emission in a Red Fluorescent Protein. Protein Sci. 2009; 18:460–466. [PubMed: 19165727]
17. Faraji S, Krylov AI. On the Nature of an Extended Stokes Shift in the mPlum Fluorescent Protein. Journal of Physical Chemistry B. 2015; 119:13052–13062.
18. Yoon EK, Patrick, Lee Junghwa, Joo Taiha, Jimenez Ralph. Far-Red Emission of mPlum Fluorescent Protein Results from Excited-State Interconversion between Chromophore Hydrogen-Bonding States. Journal of Physical Chemistry Letters. 2016 In Press.
19. Joo TH, Jia YW, Yu JY, Lang MJ, Fleming GR. Third-Order Nonlinear Time Domain Probes of Solvation Dynamics. Journal of Chemical Physics. 1996; 104:6089–6108.
20. Periasamy N. Heterogeneity of Fluorescence Determined by the Method of Area-Normalized Time-Resolved Emission Spectroscopy. Fluorescence Spectroscopy. 2008; 450:21–35.
21. Cranfill PJ, Sell BR, Baird MA, Allen JR, Lavagnino Z, Gruiter H. M. d. Kremers G-J, Davidson MW, Ustione A, Piston DW. Quantitative Assessment of Fluorescent Proteins. Nature Methods. 2016; 13:557–562. [PubMed: 27240257]

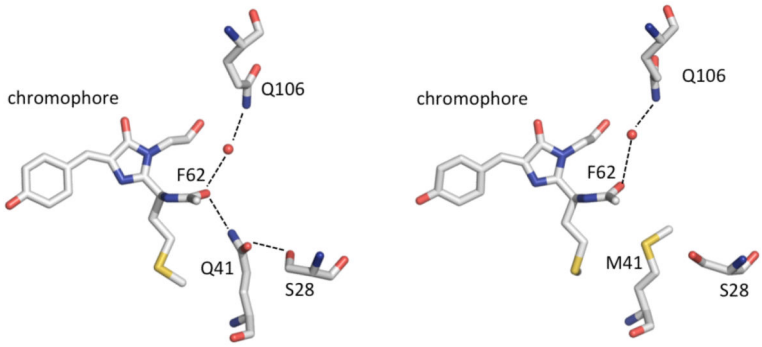

Figure 1.

Chromophore N-acylimine region from the crystal structures of (left) TagRFP675 (PDB 4KGF) and (right) mKate (PDB 3BXB). Hydrogen bonds are represented as dashed black lines; atoms are colored by atom type; water molecules are shown as red spheres.

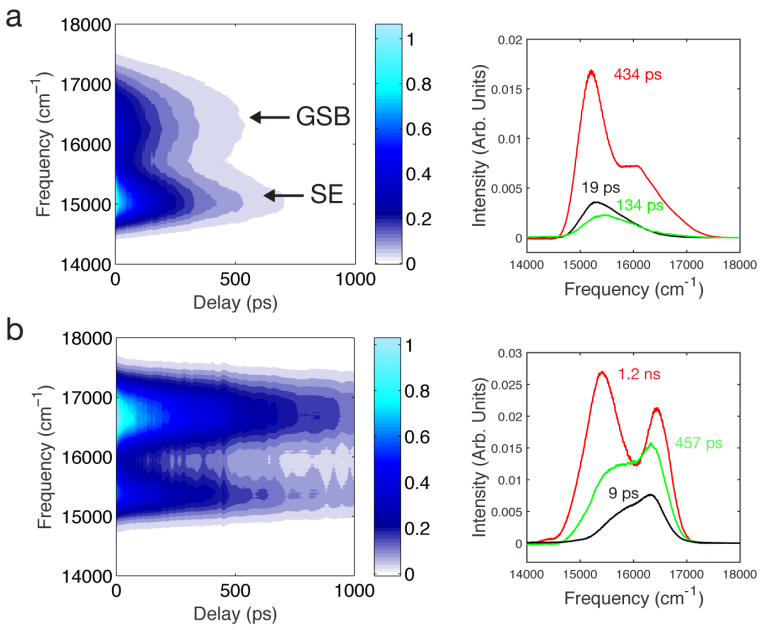

Figure 2.
SRTG spectra and DAS for (a) TagRFP675 and (b) mKate/M41Q.

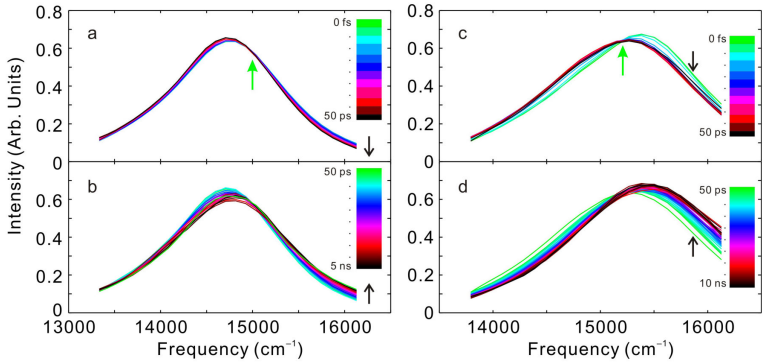

Figure 3.

TRANES spectra constructed from femtosecond and picosecond TRFS (a) TagRFP675 from 0 to 50 ps and (b) TagRFP675 from 50 ps to 5 ns (c) mKate/M41Q from 0 to 50 ps and (d) mKate/M41Q from 50 ps to 10 ns. Actual times for each curve can be obtained from the dots in Figure S5. Time increases in the direction of the black arrows. The green arrows indicate isoemissive points.

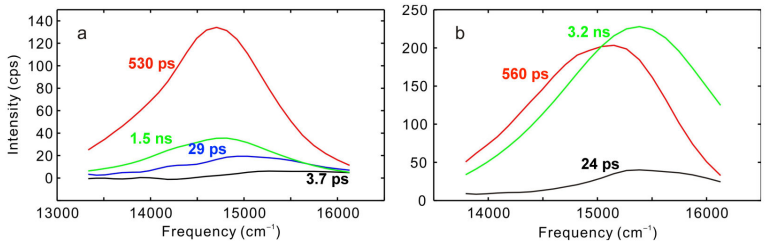

Figure 4.
DAS from global analysis of TRFS for (a) TagRFP675 and (b) mKate/M41Q.

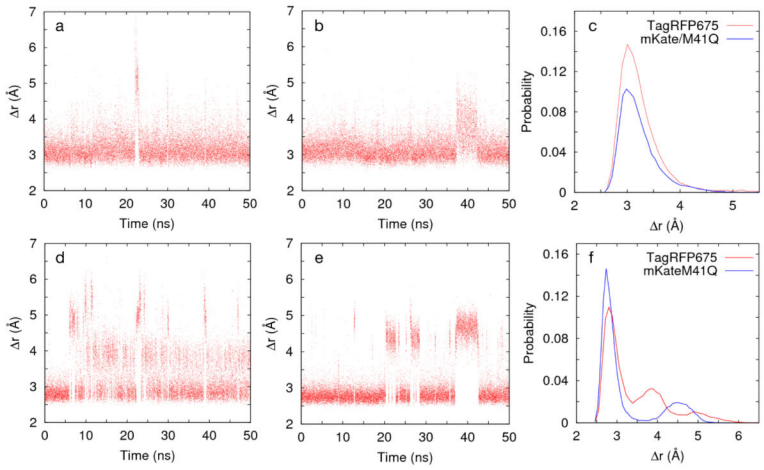

Figure 5.

Fluctuations in separation (Δ*r*) between the nitrogen atom in the sidechain of Q41 and the N-acylimine oxygen of F62 for (a) TagRFP675 and (b) mKate/M41Q. In (c), these results are given as histograms. Fluctuations of the distance (Δ*r*) between oxygen atoms in the sidechains of S28 and Q41 for (d) TagRFP675 and (e) mKate/M41Q. In (f), these results are given as histograms, with data sorted into 50 bins over the plotted range.

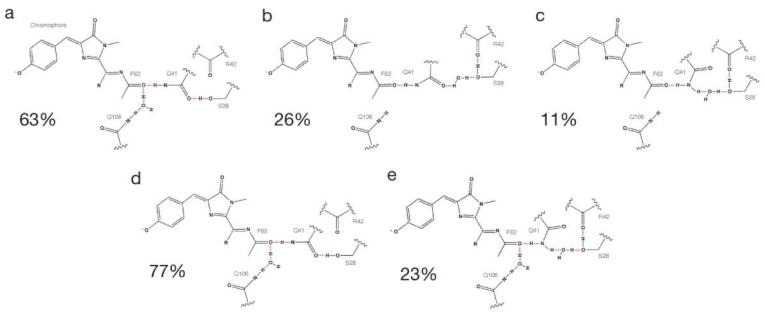

Figure 6.

Configurations of hydrogen bond network in acylimine region from MD for TagRFP675 (a-c) and for mKate/M41Q (d,e). Percentages were calculated based on the O-O distance between S28 and Q41. The three states in TagRFP675 correspond to $\Delta r<3.5$ Å, $3.5\text{Å} \leq \Delta r<4.5$ Å and $\Delta r \geq 4.5$ Å. In mKate/M41Q, the two states correspond to $\Delta r<3.5$ Å and $\Delta r \geq 3.5$ Å.

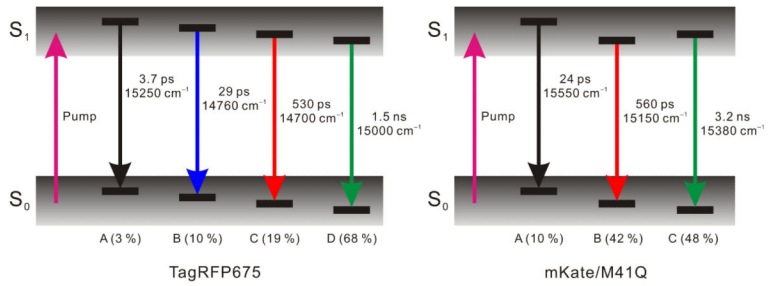

Figure 7.

Level diagrams describing photophysics of TagRFP675 and mKate/M41Q. Initial photoexcitation from a distribution of conformers in S_o creates excited-state populations with a distribution of conformers. Relative populations are noted.

Table 1

Steady state absorption and emission data for mKate and TagRFP675 variants.

Mutant	Absorption Peak (cm^{-1})	Emission Peak (cm^{-1})	Stokes Shift (cm^{-1})
mKate	17010	15750	1260
mKate/M41Q	17270	15310	1960
TagRFP675	16670	14810	1860
TagRFP675/F62A	16720	15200	1520
TagRFP675/Q106M	16950	15430	1520
Tag RFP675/F62A/Q106M	17010	15580	1430
TagRFP675/Q41M	16950	15550	1400